JACC: CARDIOVASCULAR IMAGING VOL. 5, NO. 7, 2012

ISSN 1936-878X/$36.00
PUBLISHED BY ELSEVIER INC. http://dx.doi.org/10.1016/j.jcmg.2012.03.011

Geometric Assessment of Asymmetric Septal Hypertrophic Cardiomyopathy by CMR

Anca Florian, MD,* Pier Giorgio Masci, MD,†‡ Stijn De Buck, PhD,§
Giovanni Donato Aquaro, MD,† Piet Claus, PhD,‖ Giancarlo Todiere, MD,†
Johan Van Cleemput, MD, PhD,‖ Massimo Lombardi, MD,† Jan Bogaert, MD, PhD*
Leuven, Belgium; and Pisa, Italy

OBJECTIVES The aim of this study was to analyze the geometric pattern of hypertrophy (HT) in patients with asymmetrical septal hypertrophic cardiomyopathy (HCM) using cardiac magnetic resonance (CMR) and to test the hypothesis that at least in some patients, the HT follows a longitudinal spiral pattern.

BACKGROUND The highly heterogeneous phenotypic expression of HCM is a well-known phenomenon. CMR has emerged as a robust 3-dimensional (3D) tomographic imaging technique that is increasingly used to explore phenotypic expression.

METHODS Short-axis cine CMR was used to study the 3D extent of HT (i.e., radial, circumferential, and longitudinal extent, as well as the relation between circumferential and longitudinal extent). Inclusion criteria were septal wall thickness (WT) $\geq$15 mm and septal to free wall WT ratio $>$1.3.

RESULTS CMR was performed in 132 patients. Maximal WT was 22 $\pm$ 5 mm, with a circumferential extent of 131 $\pm$ 51°, and a longitudinal extent of 64 $\pm$ 19%, resulting in a hypertrophied left ventricular (LV) surface of 26 $\pm$ 15%. Linear regression analysis showed in 86% of patients a consistent course of HT along the longitudinal direction. The HT invariably started at the basal anteroseptum and rotated, except in 2 patients, in a counterclockwise direction (CC-spiral patients) with a mean global rotation of 116 $\pm$ 68° (range 5° to 350°). After the CC-spiral patients were divided according to magnitude of rotation quartiles (Q1: 5° to 70°, Q2: 75° to 105°, Q3: 110° to 150°, and Q4: 155° to 350°), Q4 patients were significantly older and had more LV outflow tract obstruction and hypertension than patients without the spiraling pattern. In 11 patients, continuation of HT into an apical form of HCM was found.

CONCLUSIONS Using 3D analysis, we found that the majority of patients with asymmetrical septal HCM in fact showed a spiral pattern of HT following a counterclockwise (or "left-handed") spiral trajectory. The variation in magnitude of rotation among patients, however, was highly variable. Further research is warranted to better understand the significance of the current findings, in particular to relate them to the genetic and morphological substrate, hemodynamic consequences, and patient outcome. (J Am Coll Cardiol Img 2012;5:702–11) © 2012 by the American College of Cardiology Foundation

From the *Department of Radiology, UZ Leuven, Leuven, Belgium; †Department of Cardiac MRI, Fondazione CNR-Regione Toscana 'G. Monasterio,' Pisa, Italy; ‡Department of Cardiovascular Medicine, Fondazione CNR-Regione Toscana 'G. Monasterio,' Pisa, Italy; §Department of Electrical Engineering, UZ Leuven, Leuven, Belgium; and the ‖Department of Cardiovascular Diseases, UZ Leuven, Leuven, Belgium. This study was funded in part by a grant from Research Foundation Flanders (G.0613.09). Dr. De Buck has received research funding through the University of Leuven from Siemens Medical Solutions. All other authors have reported that they have no relationships relevant to the contents of this paper to disclose.

Manuscript received August 4, 2011; revised manuscript received March 8, 2012, accepted March 16, 2012.

Hypertrophic cardiomyopathy (HCM) is usually characterized by the presence of a nondilated, asymmetrically hypertrophied left ventricle (LV), but the phenotypic expression is highly heterogeneous (1,2). In an attempt to find clinical implications for different phenotypic expressions, pathological studies and echocardiography have been used to look at patterns of LV hypertrophy (2–4). In the last decade, cardiac magnetic resonance (CMR) has emerged as a robust imaging technique that provides detailed information about the presence, location, and distribution of hypertrophy in areas not well assessable by echocardiography (5,6).

See page 712

The first aim of this study was to describe the pattern of hypertrophy by CMR in radial, longitudinal, and circumferential directions. Second, based on CMR observations in patients with asymmetrical septal HCM, we raised and tested the hypothesis that the pattern of hypertrophy describes a counterclockwise spiral (CC-spiral) in the longitudinal direction when viewed from the LV apex along the basal to apical direction (7). Finally, we evaluated whether the longitudinal course of hypertrophy had an influence on functional, clinical, and demographic parameters.

METHODS

Study population. Of 150 patients with HCM referred for CMR between January 2007 and December 2010, asymmetrical septal HCM was diagnosed in 137 patients (n = 71 in Leuven, Belgium, and n = 66 in Pisa, Italy), based on the presence of a septal wall thickness (WT) ≥15 mm and a septal to free wall WT ratio ≥1.3 in the absence of other disease that could justify the magnitude of hypertrophy (1,2). Left ventricular outflow tract (LVOT) obstruction was defined as a peak resting gradient ≥30 mm Hg on Doppler echocardiography (8). Another 5 patients were excluded because of "end-stage" HCM (n = 4) and healed transmural anterior infarction (n = 1). The decision for genetic testing was left at the discretion of the referring clinicians. Written informed consent was obtained for all patients, and the study was approved by the local ethics review board of the hospitals.

CMR protocol and analysis. Studies were performed on 1.5-T CMR scanners using dedicated cardiac software, phased-array surface receiver coil, and electrocardiogram triggering (Online Appendix). The protocol consisted of cine imaging in the cardiac vertical and horizontal long-axis, short-axis, and 3-chamber view. In the short-axis direction, the LV was completely encompassed. Late gadolinium enhancement imaging was performed 10 to 20 min after intravenous contrast agent injection to assess the presence of myocardial fibrosis (9).

CMR studies were analyzed off-line using in-house–developed cardiac-dedicated software (Cardioviewer, UZ Leuven, Belgium), including assessment of LV volumes, mass and ejection, hypertrophy analysis, and assessment of myocardial fibrosis (Online Appendix). The extent of hypertrophy was assessed in radial, longitudinal, and circumferential direction using the short-axis cine images (Fig. 1). A modified centerline technique with 180 chords was used for assessment of end-diastolic myocardial WT (10). A short-axis slice was considered hypertrophied (i.e., H-slice) if chords had a WT ≥13 mm (≥12 mm for women) (11). A minimum of 12 positive chords were necessary to consider a short-axis slice hypertrophied, and the chord with the maximal WT was determined by the *radial extent* of hypertrophy (Fig. 2). This was performed for all short-axis slices starting with the most basal slice (defined as n°1) and was used to determine maximal WT and septal to free wall ratio per patient. The *circumferential extent* of hypertrophy, presented in degrees, was expressed as the angle between the limits of hypertrophy. The *longitudinal extent* of hypertrophy was expressed as a percentage dividing the number of H-slices by the total number of short-axis slices. The *global extent* of hypertrophy was defined as the hypertrophied endocardial surface and expressed as the percentage of total LV surface.

ABBREVIATIONS AND ACRONYMS

CC = counterclockwise
CMR = cardiac magnetic resonance
HCM = hypertrophic cardiomyopathy
LV = left ventricle/ventricular
LVOT = left ventricular outflow tract
WT = wall thickness

To test our study hypothesis, a linear regression analysis was used to evaluate the relation of hypertrophy in longitudinal and circumferential directions, thus not only taking into account the global longitudinal rotation of hypertrophy but also the rotational angle between consecutive short-axis slices, assuming that the rotational angle changes progressively as it is moving from base to apex. This was achieved by measuring the angle ("slice angle") between the geometric center of hypertrophy of an H-slice and the 0° reference defined as the intersection of the vertical long-axis view with the anterior myocardial wall (Fig. 1).

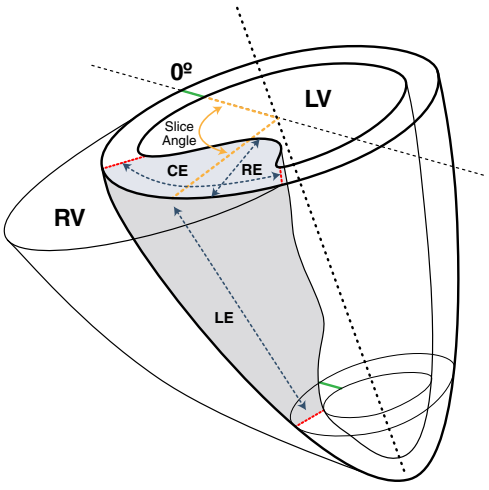

Figure 1. Scheme of Analysis of 3-Dimensional Extent of Hypertrophy

Radial extent (RE) represents maximal wall thickness (WT) per slice, circumferential extent (CE) represents the angle between limits of hypertrophy **(red lines)** per slice, and longitudinal extent (LE) represents the number of hypertrophied (H)-slices. The slice angle represents the angle between the geometric center of hypertrophy (C) and reference point (0°) (i.e., intersection of vertical long-axis [VLA] with anterior left ventricular [LV] wall **[green lines]**). RV = right ventricle.

This approach allowed spatial location of the hypertrophy and calculation of the rotation per slice (°/slice) and global rotation (°). A counterclockwise rotation was attributed a positive value (criterion 1), and an R^2 value ≥0.7 on linear regression analysis was considered to reflect a good linear fit (criterion 2). Patients fulfilling neither of the 2 criteria were classified as nonspiral (N-spiral), whereas those fulfilling both criteria were considered as having a CC-spiral pattern. Finally, in patients with concomitant concentric apical HCM, the most apical nonconcentric H-slice was used for calculation of global rotation of hypertrophy.

Statistical analysis. Continuous variables are expressed as mean ± SD. Categorical variables are expressed as frequency with percentage. One-way analysis of variance with post hoc Bonferroni analysis was used to compare continuous variable differences among patients in the N-spiral and CC-spiral groups. The chi-square test was used to compare noncontinuous variables expressed as proportions, and the Fisher exact test was used whenever 1 or more cells in the comparison table had an expected frequency of <5. The Pearson correlation (r) was used to assess the relations of demographic and clinical characteristics with hypertrophy extent. Linear regression analysis with correlation coefficient (R^2) calculation was used to test the relationship between slice angle and slice number. All tests were 2-tailed at a 5% significance level. Statistical analysis was performed using SPSS software for Windows (version 18.0, SPSS Inc., Chicago, Illinois).

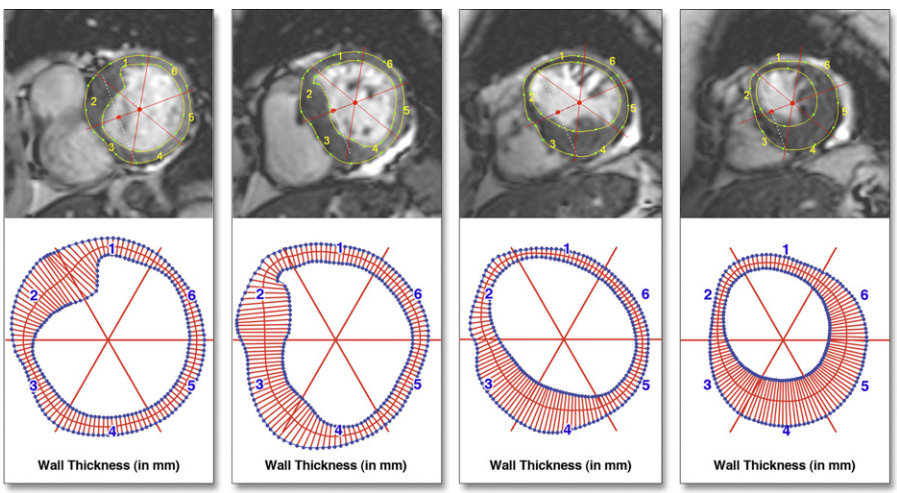

Figure 2. Modified Centerline Chord Technique to Assess Extent of Hypertrophy

Following delineation of endocardial and epicardial borders, a mid-ventricular line was defined. Next 180 chords were defined, allowing the measurement of myocardial WT. Four representative short-axis images from the LV base **(top left)** to the apex **(top right)** are shown. The **top middle panels** show the intermediate images between the LV base **(top left)** and apex **(top right)**. In the **bottom panels**, the extracted borders, mid-ventricular centerline, and the 180 chords are shown. Abbreviations as in Figure 1.

Table 1. Demographic, Clinical, Conventional, and Hypertrophy Analysis Parameters for the Studied Population (N = 132)

Age, yrs	50 ± 18
Men	94 (71)
Maximal WT (radial extent), mm	22 ± 5
Septum to free wall ratio	2.8 ± 0.7
LVOT obstruction at rest, ≥30 mm Hg	38 (29)
Concomitant apical form	13 (10)
Family SCD	26 (20)
NYHA functional class	
I	77 (58)
II	41 (31)
III–IV	14 (11)
Syncope	16 (12)
Systemic hypertension	40 (30)
LV mass, g	191 ± 68
LV mass index, g/m^2	103 ± 33
EDV, ml	150 ± 36
ESV, ml	47 ± 21
EF, %	69 ± 9
LGE presence, %	79 (60)
No. of total slices available	11 ± 1
No. of H-slices	7 ± 2
Longitudinal extent, %	64 ± 19
Circumferential extent, °	131 ± 51
Circumferential extent—nonconcentric, °	122 ± 39
Global rotation, °	103 ± 71
Hypertrophied surface, %	26 ± 15
R^2 for slice no-slice angle linear model	0.8 ± 0.2

Values are mean ± SD or n (%).
EDV = end-diastolic volume; EF = ejection fraction; ESV = end-systolic volume; H = hypertrophied; LGE = late gadolinium enhancement; LV = left ventricular; LVOT = left ventricular outflow tract; NYHA = New York Heart Association; SCD = sudden cardiac death; WT = wall thickness.

RESULTS

Patient characteristics and conventional analysis. The mean age was 50 ± 18 years (range 14 to 85 years; 71% men) (Table 1). A familial history of sudden cardiac death was present in 26 patents (20%), and 16 patients (12%) had experienced at least 1 episode of unexplained syncope. Dyspnea (New York Heart Association [NYHA] functional class II to IV) was present in 55 patients (42%). LV ejection fraction was 69 ± 9%. LVOT obstruction was present in 38 patients (29%). In 13 patients (10%), concomitant apical HCM was detected on CMR. Late gadolinium enhancement was present in 79 patients (60%). In 35 patients with genetic testing, gene mutations were found in 19 (54%).

3-dimensional extent of hypertrophy. The extent of hypertrophy was highly variable, involving 6% to 76% of the LV surface (mean 26 ± 15%). In the radial direction, maximal WT ranged between 15 and 39 mm (mean 22 ± 5 mm) with septal to free WT ratio of 1.7 to 5.6 (mean 2.8 ± 0.7) (Fig. 3A). The longitudinal extent of hypertrophy ranged between 25% and 100% (mean 64 ± 19%), but the hypertrophy initiated always in the most basal LV slices (i.e., short-axis slices 2 to 4) (Fig. 3A). No discontinuity in the longitudinal extent of hypertrophy was found. The highest WT values were found in the basal half of the LV (slices 2 to 6) (Fig. 3B). The mean circumferential extent of hypertrophy, when the concentric apical H-slides (58 slices, 7% of H-slices) were excluded, was 122 ± 39° and was fairly constant from slice 3 to 11 (Fig. 4). Circumferential discontinuity in hypertrophy was present in 11 patients involving 24 of 891 H-slices (3%).

Relation between circumferential and longitudinal extent of hypertrophy. The hypertrophy showed a longitudinal CC-spiral with a mean rotation >180°

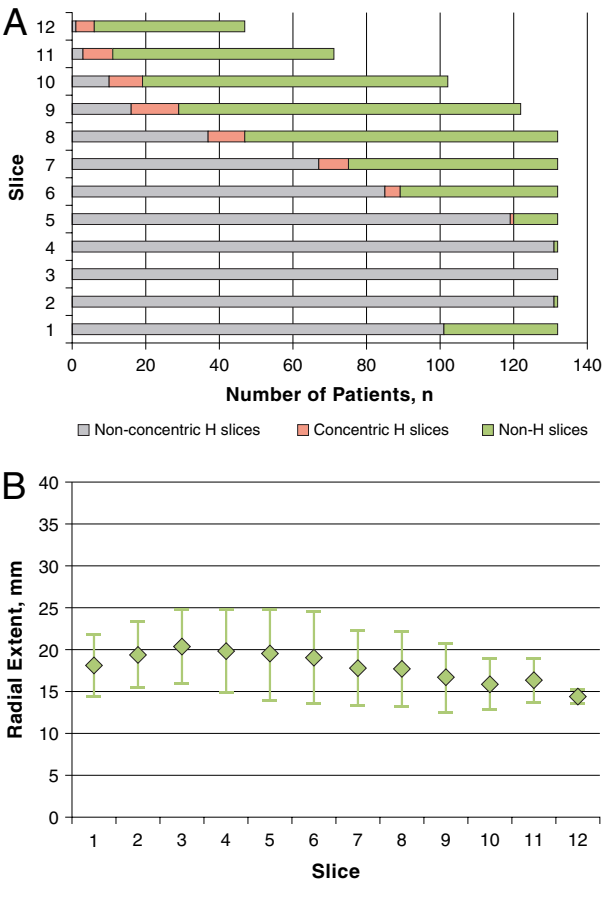

Figure 3. Longitudinal Distribution of Hypertrophy and Variation in Maximal WT per Slice

(A) Longitudinal distribution of nonconcentric and concentric H-slices and nonhypertrophied (non-H) slices. **(B)** Longitudinal variation of maximal WT per slice (i.e., radial extent). Values are shown as mean ± SD. Slice 1 is the most basal slice and slice 12 the most apical. Abbreviations as in Figure 1.

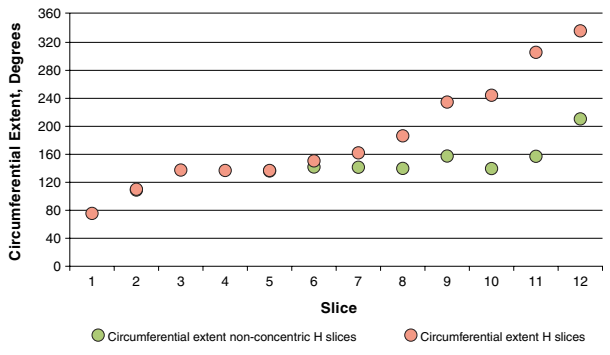

Figure 4. Circumferential Extent of Hypertrophy per Slice in Longitudinal Direction

The circumferential extent for all H-slices is shown in **red**, and the circumferential extent for nonconcentric H-slices is shown in **green**. Slice 1 is the most basal slice and slice 12 the most apical. Abbreviation as in Figure 1.

(i.e., +18 ± 20° in slice 1 to +218 ± 29° in slice 11) (Fig. 5). With 0° as the reference, the spiral started in the basal anterior to anteroseptal wall, progressed toward a more septal position for the following SA slices, and became inferoseptally or inferiorly located for the apical slices. However, as shown in Figure 5, SDs obviously increased the further away they were from the LV base, indicative of a large spread in magnitude of spiraling. Hypertrophy in LV inferolateral and anterolateral walls were found in 8% and 3% of patients, respectively (not taking into account the concentric apical forms).

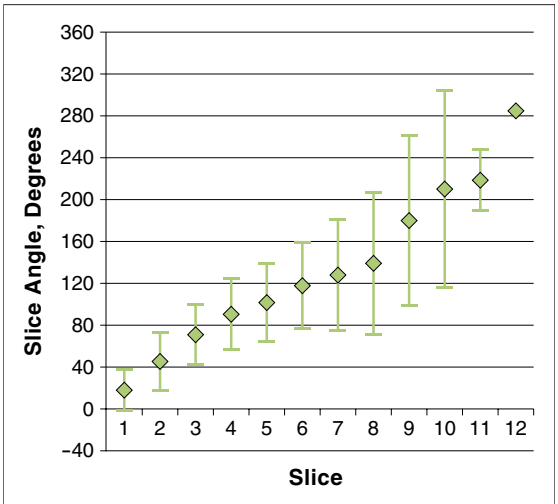

Figure 5. Variation in Mean Slice Angle of Hypertrophy in Longitudinal Direction

A close to linear increase in mean slice angle is seen from base to apex together with increasing dispersion in the same direction. Slice 1 is the most basal slice and slice 12 the most apical.

To investigate the relationship between circumferential and longitudinal extent of hypertrophy, linear regression analysis was performed. Although 18 patients showed no clear relationship ($R^2 = 0.3$) (i.e., defined as N-spiral group), the majority of patients (i.e., 114 patients [86%]) showed $R^2 \geq 0.7$ between slice angle and slice position. In 112 patients, global rotation was ≥0° (i.e., defined as CC-spiral group), whereas 2 patients showed a negative rotation of −70° and −60°, respectively. Taking into account the wide range in magnitude of rotation (range 5° to 350°, mean 116 ± 68°), CC-spiral patients were classified using quartiles, Q1: 5° to 70°, Q2: 75° to 105°, Q3: 110° to 150°, and Q4: 155° to 350° (Table 2, Fig. 6). Examples of different HCM patterns are shown in Figure 7 and Online Videos 1A, 1B, and 1C.

Relation of nonspiral/spiral patterns with demographic, clinical, and conventional CMR parameters. Global rotation was related to age ($r = 0.35$; $p < 0.0001$). In particular, Q4 CC-spiral patients (63 ± 12 years-of-age) were older than the other groups and presented a higher LV mass index ($p = 0.02$) and a higher frequency of hypertension ($p = 0.02$) (Table 2). Age, however, was not related to global, longitudinal, and circumferential extent of hypertrophy. No significant differences between groups were found regarding clinical characteristics like family history of HCM or sudden cardiac death, NYHA functional class, syncope, and prevalence of atrial fibrillation. In genetically tested patients, gene defects could not be attributed to specific phenotypic patterns, although remarkably, Q4 CC-spiral patients yielded a much lower number of positive tests than the other groups (Table 3).

Resting LVOT obstruction was more frequently present in Q4 CC-spiral patients than N-spiral patients ($p < 0.0001$), an observation that could not be explained by differences in maximal WT (i.e., radial extent) or hypertrophied surface. Remarkably, however, N-spiral patients showed more frequently late gadolinium enhancement (88%) as compared with CC-spiral groups ($p = 0.013$), whereas both groups tended to more frequently have higher scores (i.e., grades 2 to 3) of late gadolinium enhancement than the other groups. No differences in enhancement patterns were observed between groups (Table 4).

DISCUSSION

We demonstrated that the majority of patients fulfilling the criteria of asymmetrical septal HCM

Table 2. Demographic, Clinical, Conventional, and Hypertrophy Analysis Parameters for N-Spiral and CC-Spiral Groups

		CC-Spiral				
	N-spiral	Q1 (5–70°)	Q2 (75–105°)	Q3 (110–150°)	Q4 (155–350°)	p Value
n	18	28	27	29	28	
Age, yrs	41 ± 15*	46 ± 20†	48 ± 19†	50 ± 13†	63 ± 12‡	<0.0001
Men	10 (55.6)	23 (82)	19 (70)	19 (66)	21 (75)	0.4
Hypertension	2 (13)	4 (14)	7 (25)	5 (18)	16 (56)	0.02
LVOT obstruction at rest (≥30 mm Hg)	2 (13)	1 (4)*	10 (38)	8 (26)	17 (60)	<0.0001
Family HCM	8 (43)	9 (32)	9 (35)	10 (33)	8 (28)	0.9
Syncope	2 (13)	3 (12)	1 (5)	4 (13)	5 (18)	0.8
LV mass, g	186 ± 68	196 ± 74	167 ± 52	180 ± 62	221 ± 78	0.06
LV mass index, g/m^2	95 ± 30	105 ± 35	87 ± 28†	103 ± 31	121 ± 35	0.02
EDV, ml	130 ± 38	154 ± 35	148 ± 26	150 ± 37	156 ± 36	0.15
ESV, ml	39 ± 20	54 ± 23	44 ± 19	45 ± 19	48 ± 19	0.15
EF, %	71 ± 10	65 ± 9	71 ± 10	70 ± 8	70 ± 8	0.12
LGE presence	16 (88)	18 (63)	15 (56)	14 (50)	15 (54)	0.013
Septum to free wall ratio	3.4 ± 0.7	2.9 ± 0.8	2.6 ± 0.6§	2.6 ± 0.7§	2.8 ± 0.6	0.001
Radial extent, mm	26 ± 6	23 ± 5	21 ± 5§	20 ± 4§	23 ± 4	0.002
Total No. of slices, median	10.5	11	11	10	11	
Longitudinal extent, %	70 ± 18	59 ± 21	54 ± 14‡	60 ± 13	80 ± 15	<0.0001
Circumferential extent, °	147 ± 63	135 ± 66	110 ± 32	115 ± 36	151 ± 44	0.007
Hypertrophied surface, %	32 ± 19	25 ± 19†	18 ± 7*§	21 ± 9†	35 ± 13	<0.0001
Global rotation, °	26 ± 29	49 ± 19	90 ± 10	130 ± 13	205 ± 47	NA
Rotation/slice, °/slice	—	9 ± 4	17 ± 5	22 ± 6	25 ± 6	NA
R^2	0.3 ± 0.2	0.9 ± 0.07‡	0.9 ± 0.05‡	0.9 ± 0.08‡	0.9 ± 0.05‡	<0.0001

Values are mean ± SD or n (%). *p < 0.0001 versus Q4. †p < 0.05 versus Q4. ‡p < 0.0001 versus N-spiral. §p < 0.05 versus N-spiral.
CC = counterclockwise; HCM = hypertrophied cardiomyopathy; N-spiral = nonspiral; NA = not applicable; other abbreviations as in Table 1.

show a longitudinal counterclockwise ("left-handed") spiral rotation of hypertrophy. The degree of spiraling, however, is highly variable and ranges from nearly straight to highly helical. In addition, the magnitude of spiraling is positively related to age and the occurrence of LVOT obstruction. Another remarkable finding was the unexpected presence of apical hypertrophy in 10% of patients with asymmetrical septal HCM.

In agreement with previous work, we observed that magnitude and spatial extent of hypertrophy are highly variable in patients with asymmetrical septal HCM (3,4,12,13). This heterogeneity is prominent in radial and longitudinal directions, whereas circumferential extent of hypertrophy is fairly constant, involving approximately one third of the LV circumference. Hypertrophy is typically contiguous, with only 8% of patients showing discontinuity along circumferential direction, a percentage lower than reported in a previous study (13). This discrepancy is likely explained by the lower cutoff values for defining hypertrophy in our study. Geometrically, the hypertrophy usually starts in the basal anterior wall (78% of patients), and the basal anteroseptum is invariably involved, showing the greatest magnitude of hypertrophy. However, the distribution of hypertrophy is highly variable across the remainder of the LV wall, showing this heterogeneity in phenotypic expression. Assessing the relation between circumferential and longitudinal extent of hypertrophy, we found a close relation in most patients (86%), describing a longitudinal spiral trajectory. Except in 2 patients, the spiral of hypertrophy followed a counterclockwise trajectory with a mean rotation of approximately 120° but a wide range of values (5° to 350°). This corresponds to a spectrum of possible trajectories ranging from a straight longitudinal course of hypertrophy without rotation to a nearly complete helix of hypertrophy. These findings are in line with previous studies investigating the geometric pattern of hypertrophy in large HCM populations (4,13). In the work by Klues et al. (4) (n = 600), the 4 most frequent patterns of hypertrophy (representing 90% of patients) could be explained by the presence of a spiral. Recently, using CMR, Maron et al. (13) (n = 333) showed that the location of most

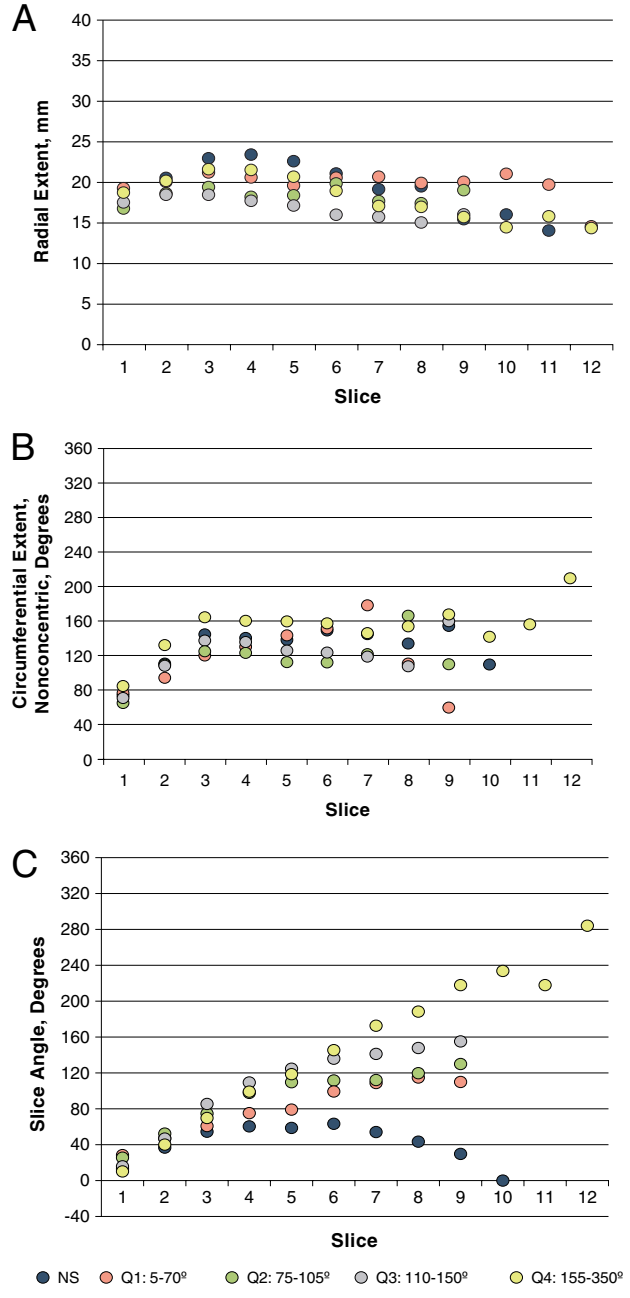

Figure 6. Differences in 3-Dimensional Extent Between N-Spiral and CC-Spiral Groups

Differences in **(A)** radial extent and **(B)** circumferential extent and differences in **(C)** slice angle values between nonspiral (N-spiral) and counterclockwise spiral (CC-spiral) groups. Slice 1 is the most basal slice and slice 12 the most apical. NS = nonspiral group.

frequently hypertrophied and thickened segments varied from base to apex (i.e., basally: anterior and anteroseptal segments; mid level: anteroseptal and inferoseptal segments; and apically: inferior and lateral segments), equally suggestive of a spiral trajectory of hypertrophy. Another interesting finding of our study was that septal hypertrophy may extend toward a complete concentric involvement of the LV apex in as many as 10% of patients, suggesting that asymmetrical septal and apical HCM are not completely separate phenotypes.

These observations give rise to several interesting questions about morphological substrate, genotype-phenotype relationship, hemodynamic consequences, and patient outcome. Notably, it should be stated that for most issues further investigation is warranted. Although the morphological substrate in HCM is well known, there is still disagreement regarding which myocardial layer is predominantly involved (14,15). In the LV wall the myofiber orientation smoothly changes from an oblique right-handed helix in the subendocardium to an oblique left-handed helix in the subepicardium. Thus, when viewed from the LV apex, the rotation of fibers is indicated by the left hand fingers for the subepicardium and vice versa for the subendocardium (16). Whereas pathological studies analyzing small ex vivo specimens hold inherent limitations to study 3-dimensionally the anisotropic structure of myocardium, diffusion-tensor CMR has become a well-validated technique for noninvasive characterization of myocardial fiber orientation. The latter technique showed that fiber disarray in patients with HCM predominantly involved the left-handed subepicardial layer of the hypertrophied septum (17). Aletras et al. (18), using displacement encoding with stimulated echoes CMR, reported an intramural functional heterogeneity, with a noncontracting subepicardial layer and largely preserved subendocardial strain in the hypertrophied areas. Thus, our finding of a CC-spiral is likely to be explained by involvement of the left-handed subepicardial layer. It can be hypothesized that the variability in observed spiral angle among patients with HCM may be caused by variation in subepicardial myofiber angle. In analogy, apical HCM may occur when the pathological fiber bundles involve the LV apex.

An inverse relationship between age and the degree of global rotation was observed. Notably, patients with extensive spiraling were significantly older, presented a higher frequency of hypertension and greater LV mass index, and remarkably had a lower number of positive tests for genetic defects. Similarly, Binder et al. (19) showed that older patients with HCM predominantly displayed a

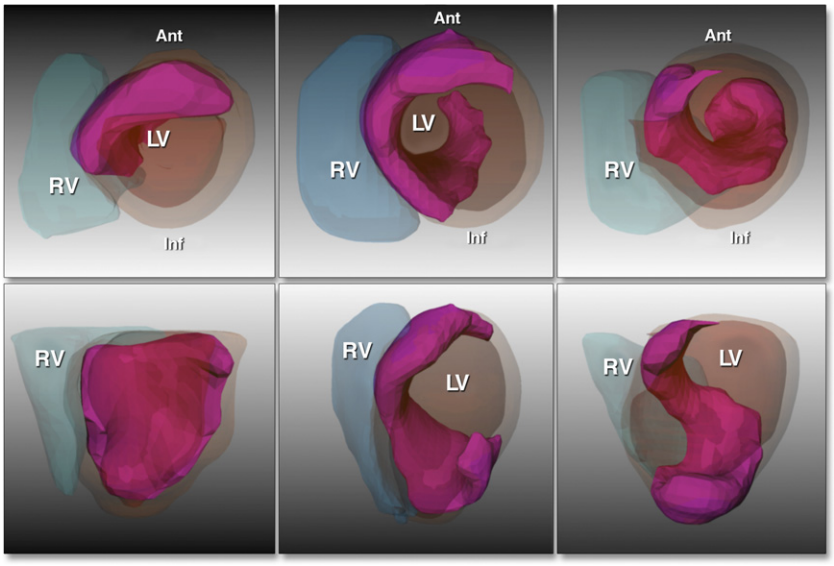

Figure 7. Volume-Rendered Images Presenting 3 Different Patterns of Spiraling

Patient with hypertrophic cardiomyopathy (HCM) with a low magnitude of spiraling and nearly straight longitudinal course of hypertrophy **(left)** (Online Video 1A), patient with HCM with a large amount of spiraling **(middle)** (Online Video 1B), and patient with spiral HCM ending in an apical form of HCM **(right)** (Online Video 1C). When viewed from the LV apex, the spiral follows a left-handed pattern (i.e., indicated by the left hand fingers), corresponding to the anatomic course of subepicardial fibers (16). Upper view **(upper panels)** and side view **(lower panels)**. Hypertrophy is shown in red. Ant = anterior; inf = inferior; RV = right ventricular; other abbreviation as in Figure 1.

sigmoid septal morphology, and they uncommonly presented genetic perturbations.

Patients with extensive spiraling more frequently showed LVOT obstruction than N-spiral patients, although there was no difference in the magnitude of hypertrophy. This finding supports that LVOT obstruction is a complex phenomenon, in which several factors other than degree of hypertrophy are involved (e.g., reduced outflow tract cross-sectional area, anterior mitral valve leaflet displacement, elongation of mitral leaflets) (20,21). It can be hypothesized that myocardial fibers in patients with extensive spiraling have a more circumferential fiber course and thus impinge more on the LVOT during cardiac contraction.

Study limitations. The current findings are strictly valid for patients with asymmetrical septal HCM and cannot be extrapolated to other HCM forms. Using septal to free wall WT ratio ≥1.3 as an additional inclusion criterion, we might have excluded HCM with laterobasal wall involvement. To evaluate the relation between circumferential and longitudinal extent of hypertrophy, we used the geometric center of hypertrophy for each short-axis slice. This center, however, does not necessarily coincide with the most hypertrophied part of the myocardium in that short-axis slice. For analysis of late gadolinium enhancement images, we used a visual, semiquantitative rather than quantitative approach. Moreover, genetic testing in larger patient groups is needed to more accurately assess the genotype-phenotype relationship. Finally, patients were studied in 2 tertiary centers in Belgium and Italy. Given the heterogeneity of HCM, it remains to be determined whether these findings are found in other HCM populations around the world.

Table 3. Genetic Testing

		CC-Spiral			
	N-Spiral	Q1 (5–70°)	Q2 (75–105°)	Q3 (110–150°)	Q4 (155–350°)
No. of tests	8	6	5	7	9
Negative	3	2	2	2	8
MYBPC3	3	2	3*	3	
MYH7	1	1	2*	2	1
CSRP3	1				
TNNT2		1			

*1 patient had 2 gene defects.
CSRP3 = cysteine- and glycine-rich protein 3; *MYBPC3* = cardiac myosin-binding protein C; *MYH7* = cardiac muscle myosin heavy chain 7 beta; *TNNT2* = troponin T type 2; other abbreviations as in Table 2.

Table 4. Frequency and Patterns of Myocardial LGE

		CC-Spiral			
	N-spiral	Q1 (5–70°)	Q2 (75–105°)	Q3 (110–150°)	Q4 (155–350°)
LGE presence	16 (88)	18 (63)	15 (56)	14 (50)	15 (54)
Grade 1/2/3	1/8/7	8/4/4	7/5/3	5/7/2	2/7/6
Location LGE					
Limited anterior	6	8	5	2	0
Limited inferior	1	1	3	2	2
Mixed anterior + inferior	3	4	4	6	10
Entire septum	2	2	0	2	1
Extensive LGE	3	3	3	2	2
+ Extension to anterior wall	2	4	0	0	4
+ Extension to apex	3	1	0	0	4

Values are n (%) or n.
Abbreviation as in Tables 1 and 2.

CONCLUSIONS

Using a CMR-based 3-dimensional analysis of hypertrophy in patients with asymmetrical septal HCM, we found a CC-spiral of hypertrophy in the majority of patients. Among patients, the magnitude of rotation, however, was highly variable. Further research is warranted to better understand the significance of the current findings, in particular to relate them to the genetic and morphological substrate, hemodynamic consequences, and patient outcome.

Reprint requests and correspondence: Dr. Jan Bogaert, Department of Radiology, UZ Leuven, Herestraat 49, B-3000 Leuven, Belgium. *E-mail: salvador.borgesneto@dm.duke.edu.*

REFERENCES

1. Maron BJ, McKenna WJ, Danielson GK, et al. ACC/ESC clinical expert consensus document on hypertrophic cardiomyopathy: a report of the American College of Cardiology Foundation Task Force on Clinical Expert Consensus Documents and the European Society of Cardiology Committee for Practice Guidelines (Committee to Develop an Expert Consensus Document on Hypertrophic Cardiomyopathy). J Am Coll Cardiol 2003;42:1687–713.
2. Hughes SE. The pathology of hypertrophic cardiomyopathy. Histopathology 2004;44:412–27.
3. Maron BJ, Gottdiener JS, Epstein SE. Patterns and significance of distribution of left ventricular hypertrophy in hypertrophic cardiomyopathy. A wide angle, two dimensional echocardiographic study of 125 patients. Am J Cardiol 1981;48:418–28.
4. Klues HG, Schiffers A, Maron BJ. Phenotypic spectrum and patterns of left ventricular hypertrophy in hypertrophic cardiomyopathy: morphologic observations and significance as assessed by two-dimensional echocardiography in 600 patients. J Am Coll Cardiol 1995;26:1699–708.
5. To ACY, Dhillon A, Desai MY. Cardiac magnetic resonance in hypertrophic cardiomyopathy. J Am Coll Cardiol Img 2011;4:1123–37.
6. Rickers C, Wilke NM, Jerosch-Herold M, et al. Utility of cardiac magnetic resonance imaging in the diagnosis of hypertrophic cardiomyopathy. Circulation 2005;112:855–61.
7. Masci PG, De Bondt J, Bogaert J. Helical form of hypertrophic cardiomyopathy: a new entity? Eur Heart J 2008;29:706.
8. Desai MY, Ommen SR, McKenna WJ, Lever HM, Elliot PM. Imaging phenotype versus genotype in hypertrophic cardiomyopathy. Circ Cardiovasc Imaging 2011;4:156–68.
9. Kim RJ, Fieno DS, Parrish TB, et al. Relationship of MRI delayed contrast enhancement to irreversible injury, infarct age, and contractile function. Circulation 1999;100:1992–2002.
10. Van Rugge PF, Van der Wall EE, Spanjersberg SJ, et al. Magnetic resonance imaging during dobutamine stress for detection and localization of coronary artery disease. Quantitative wall motion analysis using a modification of the centerline method. Circulation 1994;90:127–38.
11. Maron BJ, Pelliccia A. The heart of trained athletes. Cardiac remodeling and the risks of sports, including sudden death. Circulation 2006;114:1633–44.
12. Shapiro LM, McKenna WJ. Distribution of left ventricular hypertrophy in hypertrophic cardiomyopathy: a two-dimensional echocardiographic study. J Am Coll Cardiol 1983;2:437–44.
13. Maron MS, Maron BJ, Harrigan C, et al. Hypertrophic cardiomyopathy phenotype revisited after 50 years with cardiovascular magnetic resonance. J Am Coll Cardiol 2009;54:220–8.
14. Unverferth DV, Baker PB, Pearce LI, Lautman G, Roberts WC. Regional myocyte hypertrophy and increased interstitial myocardial fibrosis in hypertrophic cardiomyopathy. Am J Cardiol 1987;59:932–6.
15. Hoshino T, Fujiwara H, Kawai C, Hamashima Y. Myocardial fiber diameter and regional distribution in the ventricular wall of normal adult hearts, hypertensive hearts and hearts with hypertrophic cardiomyopathy. Circulation 1983;67:1109–16.

16. Sengupta PP, Tajik AJ, Chandrasekaran K, Khandheria BK. Twist mechanics of the left ventricle: principles and application. J Am Coll Cardiol Img 2008;1:366–79.
17. Tseng WY, Dou J, Reese TG, Wedeen VJ. Imaging myocardial fiber disarray and intramural strain hypokinesis in hypertrophic cardiomyopathy with MRI. J Magn Reson Imaging 2006;23:1–8.
18. Aletras AH, Tilak GS, Hsu LY, Arai AE. Heterogeneity of intramural function in hypertrophic cardiomyopathy: mechanistic insights from MRI late gadolinium enhancement and high-resolution DENSE strain maps. Circ Cardiovasc Imaging 2011;4:425–34.
19. Binder J, Ommen SR, Gersch BJ, et al. Echocardiography-guided genetic testing in hypertrophic cardiomyopathy: septal morphological features predict the presence of myofilament mutations. Mayo Clin Proc 2006;81:459–67.
20. Maron MS, Olivotto I, Harrigan C, et al. Mitral valve abnormalities identified by cardiovascular magnetic resonance represent a primary phenotypic expression of hypertrophic cardiomyopathy. Circulation 2011;124:40–7.
21. Maron BJ, Maron MS, Wigle D, Braunwald E. The 50-year history, controversy, and clinical implications of left ventricular outflow tract obstruction in hypertrophic cardiomyopathy: from idiopathic hypertrophic subaortic stenosis to hypertrophic cardiomyopathy. J Am Coll Cardiol 2009;54:191–200.

Key Words: cardiac magnetic resonance ■ hypertrophic cardiomyopathy.

APPENDIX

For additional information on CMR sequence details and extended description of hypertrophy analysis and supplementary videos, please see the online version of this article.